Supplementary Materials

Revealing the Transmission Dynamics of COVID-19: A Bayesian Framework for R_t Estimation

Xian Yang, Shuo Wang, Yuting Xing, Ling Li, Richard Yi Da Xu,
Karl J. Friston and Yike Guo

Contents

1 Mathematical Models

1.1 Time-varying Renewal Process

Origin of Instantaneous Reproduction Number R_t. Both compartment models and time-since-infection models originate from the work of Kermack and McKendrick[1] and can be unified in the same mathematical framework[2]. Let us denote the numbers of susceptible and recovered individuals at calendar time t by $S(t)$ and $U(t)$ (recovered individuals are not denoted as $R(t)$ to avoid confusion with reproduction number). Taking account of different phases of the infection period, we denote the number of infected individuals with an infection-age τ by $i(t,\tau)$. Thus, the overall number of currently infected individuals at time t is $I(t) = \int_0^t i(t,\tau)\,d\tau$ and the incident infection at time t is $j(t) = i(t,0)$. Governing equations of the homogenous transmission[2] are:

$$\frac{dS(t)}{dt} = -\lambda(t)S(t) \tag{S1}$$

$$\left(\frac{\partial}{\partial t} + \frac{\partial}{\partial \tau}\right) i(t,\tau) = -\gamma(t)i(t,\tau) \tag{S2}$$

$$\frac{dU(t)}{dt} = \int_0^t \gamma(\tau)i(t,\tau)\,d\tau \tag{S3}$$

$$i(t,0) = \lambda(t)S(t) \tag{S4}$$

where $\lambda(t)$ is the rate at which susceptible individuals get infected at time t. This is given by the infection rates per single infected individual $\beta(\tau)$ with an infection-age τ and the number of infected individuals $i(t,\tau)$ as:

$$\lambda(t) = \int_0^t \beta(\tau)\, i(t,\tau)\,d\tau \tag{S5}$$

Similarly, $\gamma(\tau)$ is defined as the recovery rate with at infection-age τ. By simplifying Equation (S2) on the characteristic line ($t = \tau + c$), we have:

$$\frac{di(\tau+c,\tau)}{d\tau} = -\gamma(\tau)i(\tau+c,\tau) \tag{S6}$$

The solution to this ordinary differential equation is:

$$i(\tau+c,\tau) = i(c,0)\mathcal{T}(\tau) \tag{S7}$$

where

$$\mathcal{T}(\tau) = exp\left(-\int_0^{\tau} \gamma(\sigma)\, d\sigma\right) \tag{S8}$$

Thus we can link the infections with infection-age τ at time t to the incident infection at time $t-\tau$:

$$i(t,\tau) = \mathcal{T}(\tau)\, i(t-\tau, 0) \tag{S9}$$

By substitute Equation (S5) and (S9) into Equation (S4), the incident infection $j(t)$ at time t is

$$j(t) = \int_0^{t} S(t)\, \beta(\tau)\, \mathcal{T}(\tau)\, j(t-\tau) d\tau \tag{S10}$$

Then we have the infectiousness profile $\beta(t,\tau)$, representing the effective rate at which an infectious individual with infection-age τ produces secondary cases at time t:

$$\beta(t,\tau) = S(t)\, \beta(\tau)\, \mathcal{T}(\tau) \tag{S11}$$

The corresponding instantaneous reproduction number $R(t)$ is derived from the integral of infectiousness profile $\beta(t,\tau)$:

$$R(t) = \int_0^{\infty} \beta(t,\tau) d\tau \tag{S12}$$

It is the average number of people that someone infected at time t is expected to infect, if conditions remain unchanged (i.e. susceptible population, infectiousness rate, recovery rate).

From the above derivation, we observe that the infectiousness profile $\beta(t,\tau)$ and corresponding instantaneous reproduction number R_t are composed of three factors: $S(t)$, $\beta(\tau)$ and $\mathcal{T}(\tau)$. $S(t)$ represents the depletion of susceptible individuals: the decline of $S(t)$ will reduce the susceptible population size leading to possible herd immunity. $\beta(\tau)$ represents the infectiousness of individuals with infection-age τ. This is related to biological (e.g. viral shedding) and behavioural (e.g. contact rates) factors. $\mathcal{T}(\tau)$ represents the recovery rate of individuals with infection-age τ: faster recovery will result in shorter infectiousness period and smaller reproduction number. All three factors, $S(t)$, $\mathcal{T}(\tau)$ and $\beta(\tau)$ can be altered by the implementation of control measures along with time.

Decomposition of the Infectiousness Profile. R_t is determined by the evolution of the infectiousness profile $\beta(t,\tau)$ according to the Equation (S12). Further, the infectiousness profile $\beta(t,\tau)$ can be rewritten as:

$$\beta(t,\tau) = R(t)\, w(t,\tau) \tag{S13}$$

where $w(t,\tau) = \beta(t,\tau) / \int \beta(t,\tau) d\tau$ is called the distribution of generation time, representing the probability distribution of infection events as a function of infection-age τ. That is, the distribution of time interval between the primary infection and subsequent secondary infection. In principle, the distribution of generation time is time-varying due to the three factors in Equation (S11), which increases the complexity of parametric modelling. Most existing studies assume a time-invariant generation time distribution (i.e. $w(t,\tau) = w(\tau)$) while the introduction of control measures results in the change of $R(t)$. Under this assumption, Equation (S10) can be rewritten as:

$$j(t) = R(t) \int_0^t w(\tau)\, j(t-\tau)\, d\tau \tag{S14}$$

This is the core formula for R_t estimation from the infection data. That is,

$$R(t) = j(t) / \int_0^t w(\tau)\, j(t-\tau)\, d\tau \tag{S15}$$

Or, we can have the corresponding discretised version:

$$R_t = \frac{j_t}{\sum_{k=1}^{T_w} w_k j_{t-k}} \tag{S16}$$

where T_w is the time span of the set $\{w_k\}$. This decomposition of infectiousness profile into R_t and time-invariant generation time distribution w_k is one of the fundamental formulae for R_t estimation in existing literature (e.g. the well-known package 'EpiEstim'[3] and this paper).

1.2 Observations of the Transmission Dynamics

Formulation of the Observation Function. The infection number j_t is the ideal data source for R_t estimation according to Equation (S16). However, it is impossible to obtain the exact number of real-time infections through intensive screening. Instead, the infections are usually observed from the statistical reports of related events (i.e. epidemic curves) such as the daily report of confirmed cases, onset cases and death number. There is an inevitable delay between the infecting event occurred and being reported. That means these epidemic curves do not

reflect the current incidence of infection j_t. We clarify this by formulating the observation function of the transmission dynamics. In the framework of data assimilation, j_t is the state variable of the dynamic epidemic system and its update is driven by the parameter R_t as described by Equation (S16). The aggregated reports C_t (e.g., daily confirmed cases, deaths) are the observing results of the state variable through an observation function H:

$$C_t = H(j_t) \tag{S17}$$

where H is the observation function and C_t is the observation result.

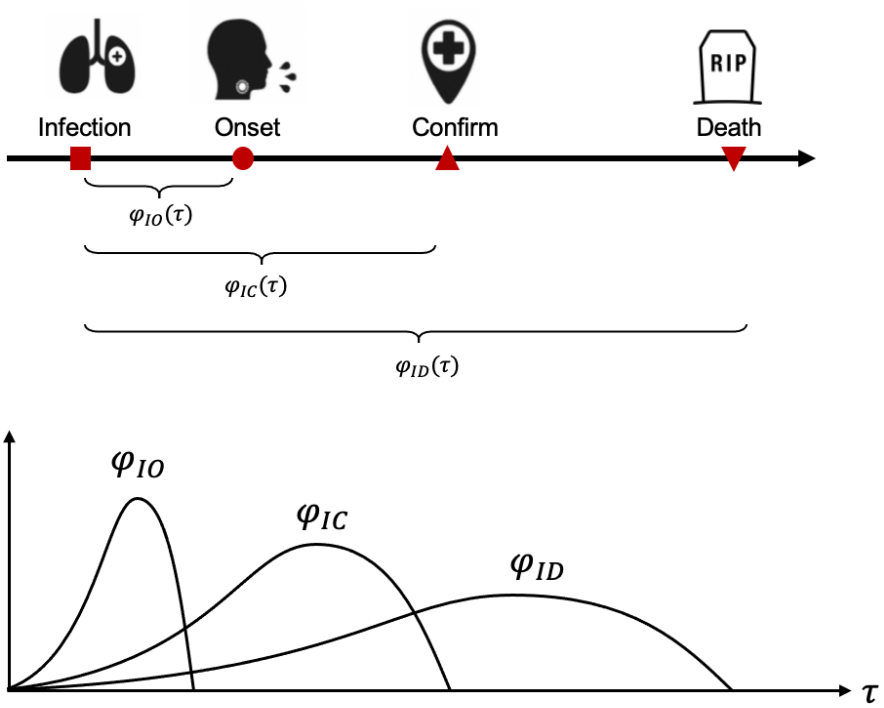

Supplementary Figure 1. Illustrations of three types of observations and corresponding distributions of time from the real infection date and observation.

Observation Functions for Various Reports. The format of the observation function H depends on the type of reported data being used. In general, H is a convolutional operation summing up the portion of infected cases weighted by the distribution of time delay between being infected and reported. Confirmed reports C_t^C, onset cases C_t^O and death reports C_t^D are the three most used reports data for R_t estimation[4–6] (illustrated in Supplementary Figure 1).

A. Onset Cases Reports. The reports of onset cases are usually compiled retrospectively from epidemic surveys of confirmed cases, which can be represented as:

$$C_t^O = \sum_{k=d_O}^{T_O} j_{t-k}\varphi_k^{IO} = \varphi^{IO} \otimes j_t \tag{S18}$$

where φ_k^{IO} is the probability that the symptom onset occurs k days after the initial infection date for a reported case, and d_O indicates the C_t^O can only cover information of infections former than d_O days. The value of d_O is determined by φ^{IO}. The distribution φ^{IO} is determined by the biological factors of the virus and has been investigated in the previous reports[7], which is considered time-independent. We use the symbol $\otimes$ to denote the convolution operation.

B. Confirmed Cases Reports. The epidemic curve of daily confirmed cases C_t^C is observed from

$$C_t^C = \sum_{k=d_C}^{T_C} j_{t-k}\varphi_k^{IC} = \varphi^{IC} \otimes j_t \tag{S19}$$

where φ_k^{IC} is the probability that a confirmed case is reported k days after the initial infection date, and d_C has a similar definition with d_O. The distribution φ^{IC} includes two parts: the time between infection to symptom onset φ^{IO}, and the time between symptom onset to reported confirmation φ^{OC}:

$$\varphi^{IC} = \varphi^{IO} \otimes \varphi^{OC} \tag{S20}$$

The former part φ^{IO} is usually similar across regions while the latter time delay φ^{OC} varies a lot due to test policies and screening capabilities[8].

C. Death Reports. The epidemic curve of death C_t^D is observed from

$$C_t^D = \rho_D \sum_{k=d_D}^{T_D} j_{t-k}\varphi_k^{ID} = \rho_D \varphi^{ID} \otimes j_t \tag{S21}$$

where ρ_D is the observed mortality rate of infected cases, φ_k^{ID} is the probability that a confirmed case is reported dead k days after the initial infection date, and d_D has a similar definition with d_O. ρ_D and φ^{ID} vary among different countries and periods due to capacities of treatment[5].

2 Model Inference

2.1 Problem Formulation

The time-varying renewal process can be formulated through the framework of state space hidden Markov models. The instantaneous reproduction number R_t and daily incident infections j_t are the two latent variables of the state space models, whose dependence is described by Equation (S16). Consider two evolution modes of R_t: emerging smooth changes when interventions are being steadily introduced/relaxed, and undergoing an abrupt change due to intensive interventions (e.g., lockdown). We introduce another latent variable M_t to automate the switch between these two modes, which will be discussed in detail in the next section. The observations C_t are the observed results of j_t through Equation (S18), (S19) and (S21). We are interested in inferring the evolution of R_t (along with j_t and M_t) upon the real-time update of observations C_t.

2.2 Inference Aims

As revealed in Equation (S14) and Equation (S17), the observations experience time delay with respect to the update of the latent state, due to the lagging and averaging effects of convolution in Equation (S18)-(S21). Thus, the changes of R_t cannot be reflected in time, due to the existence of incubation time and observation delay. In other words, accurate estimation of R_t at time t relies on future observations, which imposes the challenges of timely estimation. Therefore, we focus on two inference aims:

1. Given the latest observation, how to give a near real-time estimate of R_t and – equally if not more important – how to assess the uncertainty of the results?
2. Upon update of the real-time observations, how to modify estimations at all previous time steps and assess the uncertainties to make them more accurate taking into account the new information?

These two aims correspond to the two fundamental questions in Bayesian updating, namely the **filtering** and **smoothing** problems to be discussed in the next section.

2.3 Bayesian Updating Scheme

$\boldsymbol{X}_t =< R_{t^*}, \boldsymbol{J}_{t^*}, M_{t^*} >$ is defined as the latent state observed by C_t at time t. Since there is a delay between observation and infection, we suppose the most recent infection that can be observed by C_t is at the time $t^* = t - d$, where d is a constant determined by the distribution

of observation delay. Suppose T_φ is the length of the vector $\boldsymbol{J}_{t^*} = [j_{t^*-T_\varphi+1}, j_{t^*-T_\varphi+2}, \cdots, j_{t^*}]$ such that C_t is only relevant to $\boldsymbol{J}_{t^*}$ via Equation (S18)-(S21) and j_{t^*} only depends on $\boldsymbol{J}_{t^*-1}$ via the renewal process. We formulate the estimate of the latent state $\boldsymbol{X}_t$ from the observed reports C_t as a data assimilation problem. A sequential Bayesian approach is adopted to infer time-varying latent state, which are composed of two phases: forward filtering and backward smoothing.

Forward filtering: A sequential Bayesian updating approach is employed to infer the latest latent state from the real-time observations. Let us denote the observation history between time 1 and t as $C_{1:t} = [C_1, C_2, \ldots, C_t]$. Given that previous estimation $p(\boldsymbol{X}_{t-1}|C_{1:t-1})$ and new observation C_t, we would like to update the estimation of $\boldsymbol{X}_t$, i.e., $p(\boldsymbol{X}_t|C_{1:t})$ following the Bayes rule:

$$p(\boldsymbol{X}_t|C_{1:t}) = \frac{p(C_t|\boldsymbol{X}_t)p(\boldsymbol{X}_t|C_{1:t-1})}{\int p(C_t|\boldsymbol{X}_t)p(\boldsymbol{X}_t|C_{1:t-1})\, d\boldsymbol{X}_t} \tag{S22}$$

where $p(\boldsymbol{X}_t|C_{1:t-1})$ is *prior* and $p(C_t|\boldsymbol{X}_t)$ is *likelihood*. The *prior* can be written in the marginalised format:

$$p(\boldsymbol{X}_t|C_{1:t-1}) = \int p(\boldsymbol{X}_t|\boldsymbol{X}_{t-1})p(\boldsymbol{X}_{t-1}|C_{1:t-1})\, d\boldsymbol{X}_{t-1} \tag{S23}$$

which utilised the Markovian properties. By substituting Equation (S23) to Equation (S22), we obtain the iterative update of $p(\boldsymbol{X}_t|C_{1:t})$ given the transition $p(\boldsymbol{X}_t|\boldsymbol{X}_{t-1})$ and *likelihood* $p(C_t|\boldsymbol{X}_t)$:

$$p(\boldsymbol{X}_t|C_{1:t}) = \frac{p(C_t|\boldsymbol{X}_t)\int p(\boldsymbol{X}_t|\boldsymbol{X}_{t-1})p(\boldsymbol{X}_{t-1}|C_{1:t-1})\, d\boldsymbol{X}_{t-1}}{\iint p(C_t|\boldsymbol{X}_t)\int p(\boldsymbol{X}_t|\boldsymbol{X}_{t-1})p(\boldsymbol{X}_{t-1}|C_{1:t-1})\, d\boldsymbol{X}_{t-1}d\boldsymbol{X}_t} \tag{S24}$$

The *likelihood* can be calculated assuming an observation with Gaussian variance:

$$p(C_t|\boldsymbol{X}_t) \sim \mathcal{N}(H(\boldsymbol{X}_t), {\sigma_C}^2) \tag{S25}$$

where H is chosen accordingly to the types of reports and ${\sigma_C}^2$ is the variance of observation error that can be approximated empirically (detailed settings can be found in Supplementary Section 4). As the likelihood function has explicitly considered observation noise, it is more robust to noise compared to Poisson likelihood (used in EpiEstim). The results of using the Poisson likelihood for the same synthesised data as in Figure 3 are shown in Supplementary Figure 2, showing the benefits of considering observation noise in the likelihood.

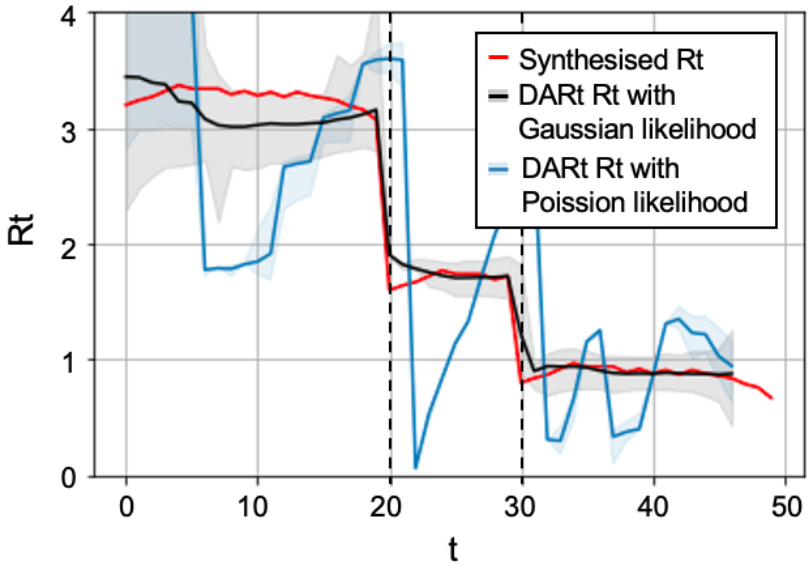

Supplementary Figure 2. Comparison between the simulation results using Poisson likelihood and Gaussian likelihood in DARt (both with 95% CI).

Then we present the $p(\boldsymbol{X}_t|\boldsymbol{X}_{t-1})$, i.e., the transition of the latent state $\boldsymbol{X}_t =< R_{t^*}, , \boldsymbol{J}_{t^*}, M_{t^*} >$ in details through analysing the evolution patterns of R_{t^*}. When R_{t^*} is evolving with smooth changes, we use a Gaussian random walk to model this pattern, named Mode I corresponding to $M_{t^*} = 0$. Under this mode, it is expected that R_{t^*} is similar to the previous time R_{t^*-1}. In contrast, the evolution of R_{t^*} can be altered significantly when intensive measures are induced. For example, R_{t^*} may experience an abrupt decrease due to the lockdown policy on time t^*. Under this circumstance, the epidemic history does not provide much information about the latest R_{t^*}, where we name it as Mode II corresponding to $M_{t^*} = 1$.

Formally, the evolution of R_{t^*} is described by the switching dynamics conditioned on M_{t^*}:

$$p(R_{t^*}|R_{t^*-1}) \sim \begin{cases} \mathcal{N}(R_{t^*-1}, {\sigma_R}^2) & M_{t^*} = 0 \quad \text{Mode I} \\ \mathrm{U}[0, R_{t^*-1} + \Delta] & M_{t^*} = 1 \quad \text{Model II} \end{cases} \tag{S26}$$

where $\mathcal{N}(R_{t^*-1}, {\sigma_R}^2)$ is a Gaussian distribution with the mean value of R_{t^*-1} and variance of ${\sigma_R}^2$, describing the random walk with the randomness controlled by σ_R. $\mathrm{U}[0, R_{t^*-1} + \Delta]$ is a uniform distribution between 0 and $R_{t^*-1} + \Delta$ allowing abrupt decrease while limiting the amount of increase. This is because we assume that R_{t^*} can undergo a big decrease when intervention is introduced but it is unlikely to have a dramatic increase in one day as the characteristics of disease would not change instantly. One exception is that for the regions whose daily infection remains as low as around 0 after the intervention, and an imported super-

spreader triggers a new outbreak. The R_{t^*} value which was remained at a low level would increase significantly. In this case, like the most recent outbreak in Hong Kong in November, we set Δ to be a large value, allowing an abrupt increase.

In our model, we assume a discrete Markovian chain process for M_{t^*} with the transition probabilities listed in Supplementary Table 1, meaning that the probability of having an abrupt change in R_{t^*} is low. This assumption is realistic as most of the time the R_{t^*} curve is undergoing smooth change.

Supplementary Table 1. Transition probabilities of M_{t^*}.

	$M_{t^*} = 0$	$M_{t^*} = 1$
$M_{t^*-1} = 0$	0.95	0.05
$M_{t^*-1} = 1$	0.95	0.05

Finally, we use the renewal process to provide transition of $\boldsymbol{J}_{t^*+1}$:

$$p(\boldsymbol{J}_{t^*}|\boldsymbol{J}_{t^*-1}, R_{t^*}) = Poisson(j_{t^*};\ R_{t^*} \sum_{k=1}^{T_w} w_k\, j_{t^*-k}\,) \prod_{m=1}^{T_\varphi - 1} \delta(\boldsymbol{J}_{t^*}^{(m)}, \boldsymbol{J}_{t^*-1}^{(m+1)}) \qquad \text{(S27)}$$

where $\boldsymbol{J}_{t^*}^{(m)}$ is the m-th component of the latent variable $\boldsymbol{J}_{t^*}$ and $\delta(x, y)$ is the Kronecker delta function. j_{t^*} is assumed to be drawn from a Poisson distribution with the mean equal to the prediction from the renewal process using R_{t^*} and $\boldsymbol{J}_{t^*-1}$. The overlaps between $\boldsymbol{J}_{t^*-1}$ and $\boldsymbol{J}_{t^*}$ are $\left\{\boldsymbol{J}_{t^*}^{(m)}\right\}_{m=1}^{T_\varphi - 1} = \left\{\boldsymbol{J}_{t^*-1}^{(m+1)}\right\}_{m=1}^{T_\varphi - 1} = [j_{t^*-T_\varphi+1}, \dots, j_{t^*-1}]$, whose distributions are assumed to be consistent. By substituting Equation (S26) and (S27) and Supplementary Table 1 into Equation (S24), we have realised the sequential Bayesian update of the latent state $\boldsymbol{X}_t =< R_{t^*}, \boldsymbol{J}_{t^*}, M_{t^*} >$ for filtering.

Backward smoothing: To answer the second question that how to update previous estimations when more subsequent observations are available, we formulate it as a smoothing problem in the Bayesian updating framework. Based on the filtering results of $p(\boldsymbol{X}_t|C_{1:t})$, we can further achieve the smoothing results $p(\boldsymbol{X}_t|C_{1:T})$, where T is the time index of the last observation. To integrate the information from the subsequent observations, we use the backward pass method. First, the joint distribution $p(\boldsymbol{X}_1, \dots, \boldsymbol{X}_T|C_{1:T})$ is decomposed as:

$$p(\boldsymbol{X}_1, \dots, \boldsymbol{X}_T | C_{1:T}) = p(\boldsymbol{X}_T | C_{1:T}) \prod\nolimits_{t=1}^{T} p(\boldsymbol{X}_t | \boldsymbol{X}_{t+1}, C_{1:T})$$

$$= p(\boldsymbol{X}_T | C_{1:T}) \prod\nolimits_{t=1}^{T} p(\boldsymbol{X}_t | \boldsymbol{X}_{t+1}, C_{1:t}) \quad \text{(S28)}$$

where

$$p(\boldsymbol{X}_t | \boldsymbol{X}_{t+1}, C_{1:t}) = \frac{p(\boldsymbol{X}_{t+1} | \boldsymbol{X}_t) p(\boldsymbol{X}_t | C_{1:t})}{p(\boldsymbol{X}_{t+1} | C_{1:t})}. \quad \text{(S29)}$$

Then by integrating out $\boldsymbol{X}_1, \dots \boldsymbol{X}_{t-1}, \boldsymbol{X}_{t+1}, \boldsymbol{X}_T$ in Equation (S28)

$$p(\boldsymbol{X}_t | C_{1:T}) = p(\boldsymbol{X}_t | C_{1:t}) \int p(\boldsymbol{X}_{t+1} | \boldsymbol{X}_t) \frac{p(\boldsymbol{X}_{t+1} | C_{1:T})}{p(\boldsymbol{X}_{t+1} | C_{1:t})} d\boldsymbol{X}_{t+1} \quad \text{(S30)}$$

which provides the iterative calculation of $p(\boldsymbol{X}_t | C_{1:T})$ from time T backwards to time t.

2.4 Particle Methods

The integrals in the filtering problem (Equation (S24)) and the smoothing problem (Equation (S30)) are intractable, thus we introduce a Sequential Monte Carlo (SMC) method called 'particle filter' to infer the latent state[9].

In Monte Carlo method, the continuous distribution of a random variable $X \sim \pi(x)$ is approximated by N independent samples with importance weights:

$$\pi(x) \approx \sum_{i=1}^{N} W^i \delta_{X^i}(x) \quad \text{(S31)}$$

where $\pi(x)$ is an arbitrary probability distribution and N independent samples $X^i \sim \pi(x)$ are drawn from the distribution with the normalized importance weight W^i. $\delta_{X^i}(x)$ denotes the Dirac delta mass located at the i-th sample X^i. These discrete samples are also called 'particles' in particle method, whose locations and weights are used to approximate the intractable integral.

If x is a time-dependent state variable, we can update the samples to approximate the distribution through the Sequential Importance Sampling (SIS) technique[10]. The locations and weights of the particles representing the target distribution are iteratively updated considering the new observations. For the filtering problem, we can set $p(\boldsymbol{X}_{1:t} | C_{1:t})$ as the target distribution and use N particles $\{\boldsymbol{X}_t^1, \boldsymbol{X}_t^2, \dots, \boldsymbol{X}_t^N\}$ with importance weight $\{W_t^1, W_t^2, \dots, W_t^N\}$ at time t. The SIS technique includes two steps: First, new positions of the particles $\boldsymbol{X}_t$ at time t are proposed according to a proposal function $q(\boldsymbol{X}_t | \boldsymbol{X}_{1:t-1})$ which can be the transition

probability $p(\boldsymbol{X}_t|\boldsymbol{X}_{1:t-1})$. Next, the importance weight $\omega(\boldsymbol{X}_{1:t})$ of the proposed particles are calculated according to iteration in Equation (S22):

$$\omega(\boldsymbol{X}_{1:t}) = \frac{p(\boldsymbol{X}_{1:t}|C_{1:t})}{q(\boldsymbol{X}_{1:t})} = \frac{p(\boldsymbol{X}_{1:t-1}|C_{1:t-1})}{q(\boldsymbol{X}_{1:t-1})}\frac{p(\boldsymbol{X}_t|\boldsymbol{X}_{1:t-1})p(C_t|\boldsymbol{X}_t)}{q(\boldsymbol{X}_t|\boldsymbol{X}_{1:t-1})}$$

$$= \omega(\boldsymbol{X}_{1:t-1})\frac{p(\boldsymbol{X}_t|\boldsymbol{X}_{1:t-1})p(C_t|\boldsymbol{X}_t)}{q(\boldsymbol{X}_t|\boldsymbol{X}_{1:t-1})} = \omega(\boldsymbol{X}_{1:t-1})p(C_t|\boldsymbol{X}_t) \quad \text{(S32)}$$

Therefore, the filtering results of $p(\boldsymbol{X}_{1:t}|C_{1:t})$ can be numerically approximated by the evolving particles and their importance weights. Similarly, the smoothing procedure of Equation (S30) can be approximated by the particles.

3 DARt Application to UK Cities

We applied DARt to monitor seven cities in England as shown in Supplementary Figure 3. All these cities are undergoing the second wave of COVID-19, where their R_t values are above 1 since August 2020 and keep fluctuating above 1 for most of the time. We can observe that cities within the UK have distinct R_t curves, reflecting that the country-wide R_t curve shown in Figure 4 (C) cannot be used to represent the epidemic dynamics across different local areas. In epidemic modelling, we should also make efforts to utilise data collected from local areas for fine-grained spatial modelling. On 22nd of September 2020, the UK government has enforced interventions in England. It is observed that Leeds, Sheffield, Liverpool and Manchester have a sharp decrease in R_t around that time. The probability values of having abrupt changes (green bars in Figure 4) for these cities around this day were larger than most other days, indicating the detection of abrupt changes. Most cities maintained a lower R_t level after this intervention. On 5th of November 2020, another intervention had taken place so that R_t values for most cities became lower than 1. As the amounts of decrease in R_t are within a small range, no sharp changes in R_t were observed such that the green bars in Figure 4 remained at a low level.

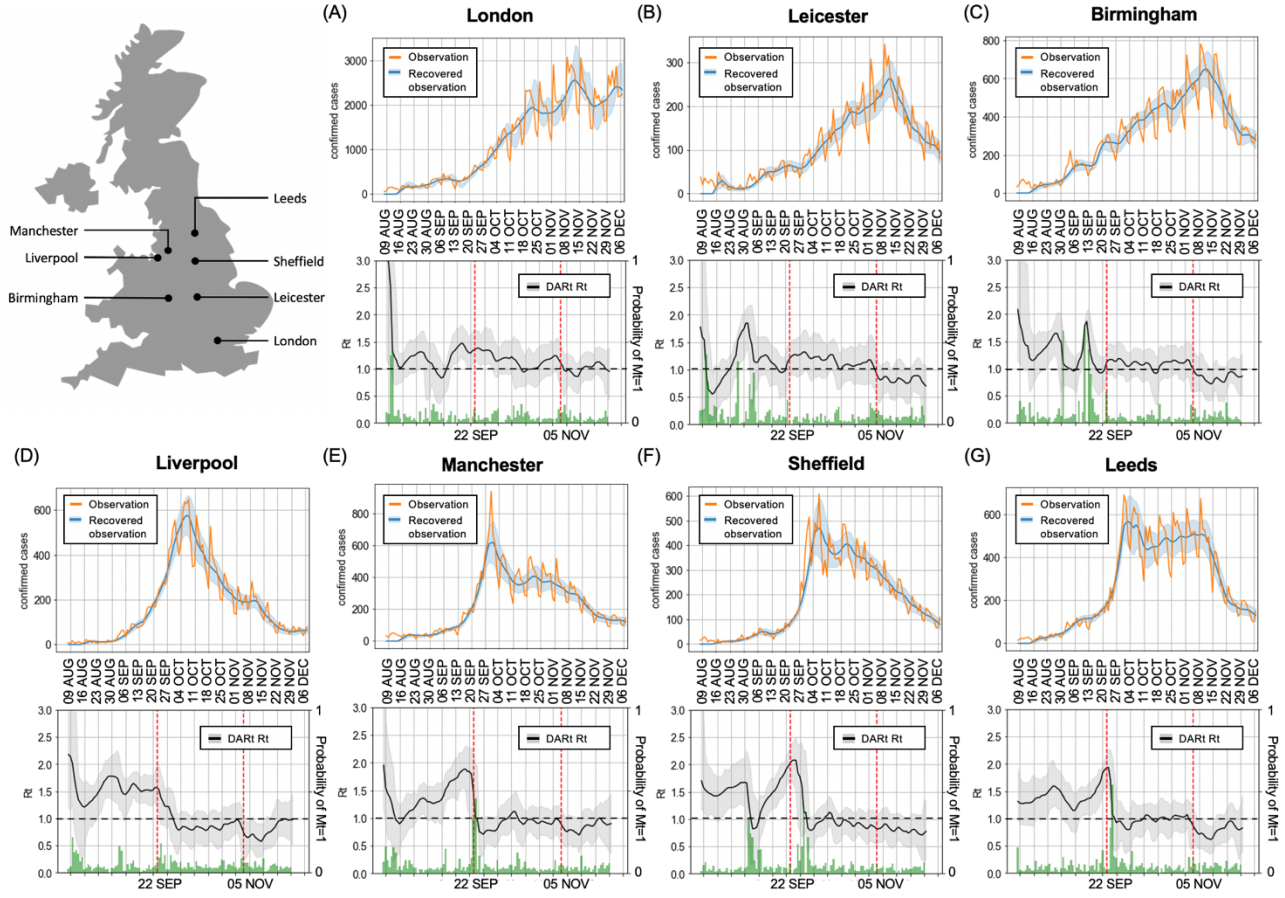

323

324 **Supplementary Figure 3.** Epidemic dynamics in London, Leicester, Birmingham, Liverpool, Manchester, Sheffield and Leeds. The top row
325 of each subplot shows the number of daily observations (in yellow) and the recovered daily observations (in blue), which validates the R_t
326 results. The bottom row shows the DARt results of R_t curve with 95% CI (in black) and the probability of having abrupt changes (i.e., $M_t =$
327 1) (in green). Two intervention dates in England are annotated in red dash lines.

4 Experimental setting

In our experiments, the generation time and observation delay distributions are adopted from the previous reports[6,8]. To truncate these distributions into a fixed length, we discard the time points with the kernel values smaller than 0.1 resulting in the length of $\boldsymbol{J}_{\mathrm{t}}$ as 7. The initial guess of R_t at $t = 0$ is set to be uniformly distributed from 1 to 5. We set $\sigma = 0.1$ for getting smooth R_t change in Model I. In Model II, we set $\Delta = 0.5$ for most regions except Hong Kong. For Hong Kong, when the average observation number of the recent 10 days is lower than 5 and the current observation number suddenly increases over 10, we think there is a chance that a newly imported case triggers a new outbreak, so we allow R_t to have an abrupt increase. In this case, we set the upper limit of R_t to be a large value which is 5 in our experiment. For implementing the particle filter, the number of particles is set to 200 for approximating distributions.

The variance of observation error ${\sigma_C}^2$ is estimated empirically. We first calculate the 7-day moving average observations. By subtracting the moving average from the observation, we obtain a difference curve, approximating random observation fluctuations. The next step is to perform the 7-day moving average calculation again on the squared value of the difference curve, where the resulted curve is regarded as the observation error variance. Finally, we use a Gaussian distribution as the likelihood function (Equation (S25)), where its variance is approximated by the observation error variance curve.

References

1. Kermack, W. O. & McKendrick, A. G. A contribution to the mathematical theory of epidemics. *Proc. R. Soc. London. Ser. A, Contain. Pap. a Math. Phys. Character* **115**, 700–721 (1927).
2. Chowell, G., Hyman, J. M., Bettencourt, L. M. A. & Castillo-Chavez, C. *Mathematical and Statistical Estimation Approaches in Epidemiology*. *Mathematical and Statistical Estimation Approaches in Epidemiology* (Springer Netherlands, 2009).
3. Cori, A., Ferguson, N. M., Fraser, C. & Cauchemez, S. A new framework and software to estimate time-varying reproduction numbers during epidemics. *Am. J. Epidemiol.* **178**, 1505–1512 (2013).
4. Pan, A. *et al.* Association of Public Health Interventions With the Epidemiology of the COVID-19 Outbreak in Wuhan, China. *JAMA* **323**, 1915 (2020).
5. Flaxman, S. *et al.* Estimating the effects of non-pharmaceutical interventions on COVID-19 in Europe. *Nature* 1–5 (2020).
6. Leung, K., Wu, J. T., Liu, D. & Leung, G. M. First-wave COVID-19 transmissibility and severity in China outside Hubei after control measures, and second-wave scenario planning: a modelling impact assessment. *Lancet* **395**, 1382–1393 (2020).
7. He, X. *et al.* Temporal dynamics in viral shedding and transmissibility of COVID-19. *Nat. Med.* (2020).
8. Ferretti, L. *et al.* Quantifying SARS-CoV-2 transmission suggests epidemic control with digital contact tracing. *Science (80-.).* **368**, eabb6936 (2020).
9. Doucet, A. & Johansen, A. M. A tutorial on particle filtering and smoothing: Fifteen years later. in *Handbook of nonlinear filtering* **12**, 3 (2009).
10. Maceachern, S. N., Clyde, M. & Liu, J. S. Sequential importance sampling for nonparametric Bayes models: The next generation. *Can. J. Stat.* (1999).